phys. stat. sol. (a) **181**, 141 (2000)

Subject classification: 68.35.Bs; 73.40.Ns; S5

Future Diamond UV Imagers For Solar Physics

J.-F. HOCHEDEZ[1]) (a), E. VERWICHTE (a), P. BERGONZO (b), B. GUIZARD (b), C. MER (b), D. TROMSON (b), M. SACCHI (c), P. DHEZ (d), O. HAINAUT (e), P. LEMAIRE (e), and J.-C. VIAL (e)

(a) Royal Observatory of Belgium, B-1180 Brussels, Belgium

(b) LETI(CEA–Technologies Avancées)/DEIN/SPE, CEA/Saclay, F-91191 Gif-sur-Yvette, France

(c) Laboratoire pour l'Utilisation du Rayonnement Electromagnétique, BP 34, F-91898 Orsay Cedex, France

(d) Laboratoire de Spectroscopie Atomique et Ionique, F-91405 Orsay Cedex, France

(e) Institut d'Astrophysique Spatiale, F-91405 Orsay Cedex, France

(Received March 2, 2000)

Despite their steady improvement over the last decades, the UV imaging detectors exhibit some limitations – inherent to their silicon technology – that become critical in the context of space missions where the highest spatial resolution, temporal cadence, and photometric accuracy are required. The use of diamond imagers would allow to overcome many of the drawbacks, opening new perspectives in particular for solar observations. It will also make the instruments cheaper. As for projects like the Solar Probe of NASA or the Solar Orbiter of ESA, the case for diamond UV detectors is even stronger, since these missions approach very near to the Sun where the temperature and the radiation fluxes are extremely high. These are the main motivations behind the new R&T programme approved by the French space agency (CNES) in August 1999 which is dedicated to demonstrate the feasability of UV imagers made of semiconducting diamond. In this paper, we report on recent experiments led at the Super-ACO synchrotron facility of LURE in the 150 to 600 eV photon energy range in order to address the influence of surface effects and electrode geometries on the detector behaviour. Quantum Efficiency (QE) values as high as 20% have been measured on prototype detectors over the investigated energy range.

1. Introduction

In August 1999, the French space agency (CNES) approved an R&T project dedicated to demonstrate the feasability of UV imagers made of semiconductor diamond. The investigation, named BOLD (Blind to the Optical Light Diamond), is carried out in France and Belgium by more than ten institutes[2]). This team gathers a broad and ex-

[1]) Corresponding author: e-mail: hochedez@oma.be

[2]) As of February 2000, they are: Institut d'Astrophysique Spatiale (IAS), Instituut voor Materiaal Onderzoek (IMO), Laboratoire d'Etudes des Propriétés Electroniques des Solides (LEPES), Laboratoire d'Electronique, de Technologies et d'Instrumentation (CEA/LETI), Laboratoire de Génie Electrique de Paris (LGEP), Laboratoire de Physique des Lasers (LPL), Laboratoire de Physique des Milieux Ionisés (LPMI), Laboratoire de Physique des Solides et de Cristallogénèse (LPSC), Laboratoire de Spectroscopie Atomique et Ionique (LSAI), Laboratoire pour l'Utilisation du Rayonnement Electromagnétique (LURE), and Royal Observatory of Belgium (ROB).

tensive expertise in the fields involved: materials growth, device design, electrical and optical characterizations, application specifications.

The performance of UV sensitive detectors has steadily increased over the last decades in many respects, and astronomical applications benefit from this evolution. These sensitive and highly linear imagers have made possible the success of recent solar missions such as SOHO, YOHKOH, TRACE, and others (see, e.g., [1]).

Nevertheless, CCDs designed for UV observations exhibit a few drawbacks that are difficult to overcome within silicon technology:

– Cooling reduces the dark current and prevents degradations from ionizing radiations, but it is a difficult and expensive solution in space missions.

– The low temperature of the detector transforms it into a cold trap for contaminants. The molecules stick to the sensitive surface and may even polymerize under the UV flux, degrading the detector performances irreversibly.

– The presence of ionizing radiations leads to images that are immediately covered by cosmics (bright points and strikes) that are hard to separate from the UV signal. Besides, the subsequent degradation of the charge transfer jeopardizes the mission life time [2].

– The existence of an evolving oxide deteriorates the quantum efficiency (QE), its stability, and its spatial homogeneity, affecting the calibration reliability.

– The minimal size of the silicon UV pixel is limited to approx. 10 μm.

– The penetration depth of the photons in the silicon determines a pan-chromatic sensitivity which is deleterious when observing a bright visible source like the Sun: one must add filters that absorb the undesired photons, but also attenuate the expected ultraviolet signal (see Fig. 1).

These drawbacks become critical in the context of solar space missions where the highest spatial resolution, temporal cadence and photometric accuracy are sought after. A significantly better spatial resolution can be achieved either by going close to the Sun with a "standard" instrument, or by increasing appreciably the aperture and the focal length of a telescope in an Earth orbit. In the first category (Solar Probe [4] and Solar Orbiter [5] missions), the whole package (including the detector) is submitted to a high radiative and particle flux. In the second case, the increase of spatial resolution happens inevitably at the expense of the signal level, especially if the temporal resolution is to be matched with the smaller observables. For instance, a resolution of tens of kilometers on the Sun (better than 0.1 arcsec) implies exposure times smaller than 1 s since expected velocities (e.g. Alfven) may be of the order of 1000 km/s.

Diamond imagers would help to circumvent many of the limitations listed above, leading to improved performances:

– The 5.5 eV bandgap permits to operate the detector at room temperature, with no need for cooling and reduced pollution risk. The bandgap also makes the diamond detector "solar-blind" (or visible-blind, i.e. insensitive to optical light, see Fig. 1). As the filters have a thermal role and because of the incomplete solar-blindness, they cannot be suppressed, but their number can be reduced, thus improving the effective area of UV instruments (and allowing shorter integration times, improved S/N, etc.).

– The compact crystal network of diamond provides radiation-hardness.

– The absence of oxide can improve the QE and its stability.

– The pixel is potentially in the sub-micrometer range, an order of magnitude smaller than achieved today.

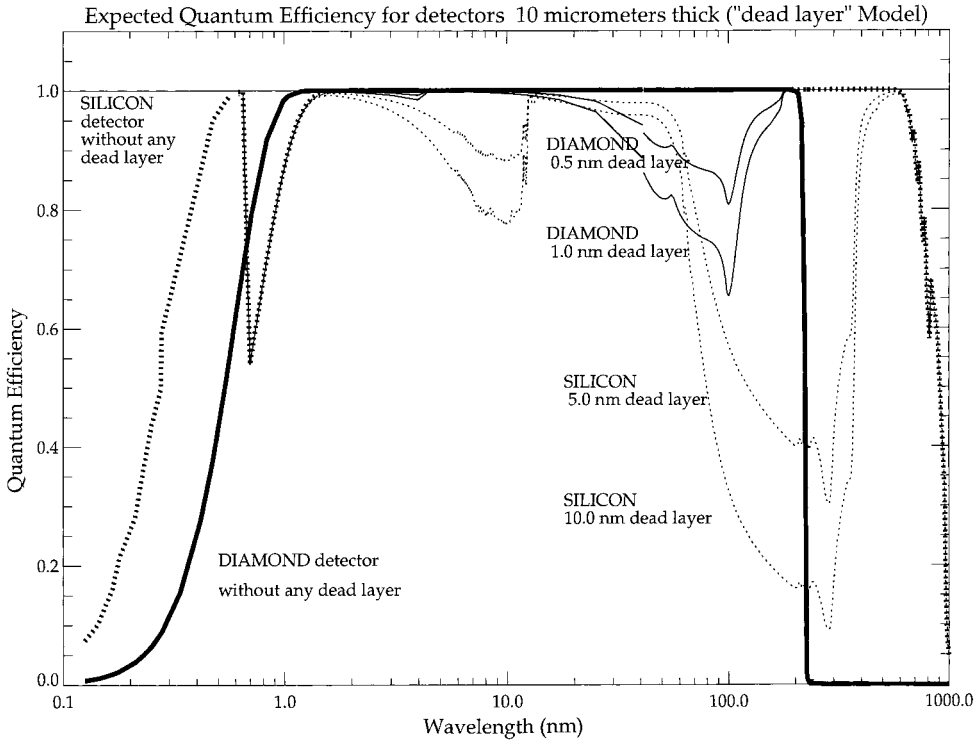

Fig. 1. Compared QE between silicon and diamond detectors estimated by a simple "dead layer" model (see [3] for better models). The plain curves correspond to diamond, the dotted curves to silicon. The thick ones show the modeled QE with no dead layer. In all instances, the depletion is 10 μm

Consequently, a diamond imager would open – just like the CCD in the past – new opportunities in the development of solar telescopes and spectrometers of higher performances. They will be more cost-effective as well by sparing the cooling hardware.

CVD diamond has been identified as an excellent material for UV detection early (see [6] and historical references in [7, 8]). Many of the contributors to BOLD not only have the appropriate testing equipment, but also find an interest in the aimed device [9 to 16]. Other teams are working in similar directions (e.g. [17 to 19]). Until now, the factor which prevented the development of such detectors has been the material quality. Therefore, the chosen strategy has been to first address meaningful parameters on the best available samples, using a well-proven technique with synchrotron XUV. This is why – although the a priori wavelength range of interest is from 100 to 2200 Å – the November 1999 measurements were done around the carbon C_K edge (289 eV, ≈43 Å) where the penetration depth of the photons spans from 100 nm to 1 μm. A channeltron collected the photo-electrons produced by the impinging synchrotron beam, in partial (PY) or total (TY) electron yield mode, in order to separate bulk and surface properties. By varying the sample preparation steps (e.g. cleaning) and the electrode geometry, some insight has been gained into the physics of the signal collection.

The remaining part of this paper is organized as follows: the experimental section describes the testing facility and the devices under study, the section on experimental

results details the main measurements, and discusses their interpretation. The conclusion presents the outlook for the various aspects of the current effort.

2. Experiments

CVD diamond membranes have been studied under XUV monochromatic light. The samples were provided by LETI/CEA and the synchrotron beam line by SACO/LURE.

2.1 Sample selection

The plasma enhanced chemical vapour deposition technique (PECVD) enables the fabrication of large area diamond layers on refractory metals or silicon from the microwave-assisted plasma dissociation of a methane and hydrogen precursor mixture. The material obtained has a polycrystalline structure with a grain size of about 10% of the layer thickness. Under optimised conditions, pure diamond can be obtained. This is revealed by Raman analysis which shows one intense peak at 1332 cm^{-1} and no other non-carbon species. The growth conditions (0.5% methane in hydrogen, and 750 °C substrate temperature) had previously been optimised in order to yield the best electronic properties [20]. Typical growth rates are of the order of 0.2 to 0.5 μm/h for this type of films (see Fig. 2).

Depending on the thickness deposited on the silicon substrate, it is possible to keep the latter to give the thin layers mechanical resistance, or to etch it in acids and use the diamond film as a free standing layer (when $\geq$ 60 μm). Membranes can also be fabricated via the etching of a hole in the silicon wafer using an $HF:HNO_3$ 1:1 acid solution. Thin layers of diamond supported by a silicon ring are obtained using this technique. At a thickness of 20 μm, an 8 mm diameter membrane has sufficient mechanical resilience to enable normal handling and transportation. Membranes as thin as 2 μm can be fabricated, but for vacuum applications, they have to be handled with care since they can easily shatter by the pressure variations encountered during rough pumping. Prior to the formation of electrical contacts, the diamond samples were annealed and chemically treated. This constitutes a critical step in the device fabrication resulting in a reduction of the device leakage current (by up to seven orders of magnitude compared to that of untreated samples) down to values below 1 pA at 50 kV/cm [21]. Gold pads 500 Å thick were deposited to form electrodes, using an e-beam evaporator. Contact geometries were obtained using the standard photolithographic techniques. At the typical operating voltages of 10^4 Vcm^{-1}, the barrier height that

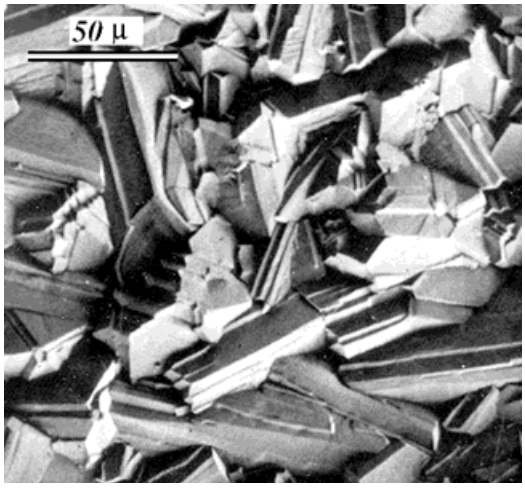

Fig. 2. Optical photograph of the diamond surface showing non-oriented crystallites

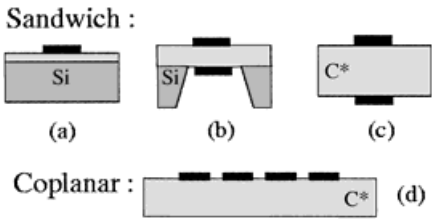

Fig. 3. Scheme of the simple configurations tested. The results presented in this paper mainly relate to the sandwich (b), and the coplanar structures (d)

results from the use of gold on diamond is negligible with respect to the bias. The membranes actually used were 20 or 200 μm thick, making the grain size of the order of a few microns.

Three main categories of electrode structure have been employed:

(i) Coplanar, interdigitated (Fig. 3d): the electrodes are deposited on the top side (last grown) and are 10 nm thick; the membrane is either 20 or 200 μm thick. The inter-electrode separation distance is 200 μm.

(ii) Coplanar, rectangular pads: two square electrodes 500 μm wide are deposited 1 mm apart on the top side.

(iii) Sandwich (Fig. 3b): the membrane is 20 μm thick, the electrodes cover both sides and are 10 to 100 nm thick.

Additionally, a graphite substrate has been made available for comparision, and for wavelength calibration purposes.

2.2 Measurement set-up

The measurements were performed during a three weeks campaign in November 1999 on the SU-7 beamline of the Super-ACO synchrotron in Orsay, France. The energy range 150 to 600 eV (20 to 80 Å), which contains the carbon K edge at about 289 eV, can be spanned by a single grating with an average resolution $E/\Delta E \approx 10^3$. The flux in the 0.5×0.5 mm^2 focal spot is of the order of 10^{12} to 10^{13} ph/s over the considered energy range.

The sample holder was designed to accomodate up to five electrically insulated diamond membranes. For each of them a bias potential (up to ± 300 V) could be applied between the electrodes. A floating picoammeter was used to measure the current flowing through the electrodes as a function of the bias potential and/or the impinging photon flux and energy.

We also measured absorption spectra across the carbon K edge, collecting with a channeltron the photoelectrons emitted by the diamond samples. A bias voltage was applied on the channeltron head, in order to select the probing depth of the absorption measurement [22]. A positive bias guarantees that all the photoemitted electrons are collected, and in particular the dominant low energy fraction that travel long distance in diamond: a probing depth in the order of 1000 Å is estimated in this case, giving bulk sensitivity. A negative bias on the channeltron head forms a high pass filter on electron energies, reducing the probing depth of the electron yield measurement [23]. We used a bias of -100 V for PY collection, leading to an estimated field of view of 20 to 30 Å, and to an increased surface sensitivity of the absorption measurement.

To summarize, the free parameters at our disposal are the photon energy, the channeltron potential, the sample polarization, and the sample selection. The measure is the channeltron count rate and/or the sample current.

3. Experimental Results

Results were obtained on the surface vs. bulk properties as a function of post-processing treatments, and on the efficiency of interdigitated devices.

3.1 Surface vs. bulk properties

Figure 4 reveals some of the surface and volume properties of the treated samples. One can clearly note a peak at 287 eV and a bulge at 289 eV in the surface spectrum that vanish in the deeper layers. The 287 eV line pertains to sp^2 graphitic-like bonds. The bulk and surface curves were normalized at the 291 eV main peak where the photon energy deposition is the shallowest. To the extent of the experiment sensitivity, the volume (500 to 1000 Å) is devoid of non-diamond bonds.

3.2 Effect of annealing and cleaning

In Figure 5, the spectra of raw and treated surfaces (PY) are compared. The 287 eV sp^2 line is seen to the left of the main 291 eV peak in both cases. The 289 eV feature is related to C–H bonds in the hydrogenated surface. It appears as a peak before processing, but is less prominent afterwards. The volume (TY) spectra are not modified by the surface processings. In a tentative preliminary conclusion, the treatments do not appear to have a very important impact on the surfaces, as seen with this probing method.

3.3 Device operation and efficiency

The I–V curve of Fig. 6 is symmetrical. This confirms the ohmic nature of the coplanar contact. The measurement was conducted under $\approx 10^{12}$ ph/s monochromatic light. Such

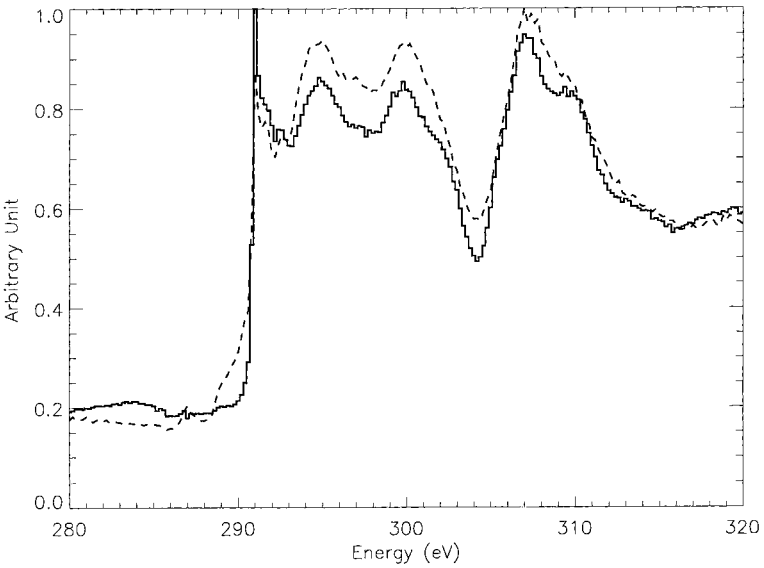

Fig. 4. Normalized channeltron counts as a function of photon energy for cleaned samples. The dashed line corresponds to surface layers (PY; $E \geq 100$ eV, i.e. 30 to 50 Å), the solid line to the volume (TY; 500 to 1000 Å)

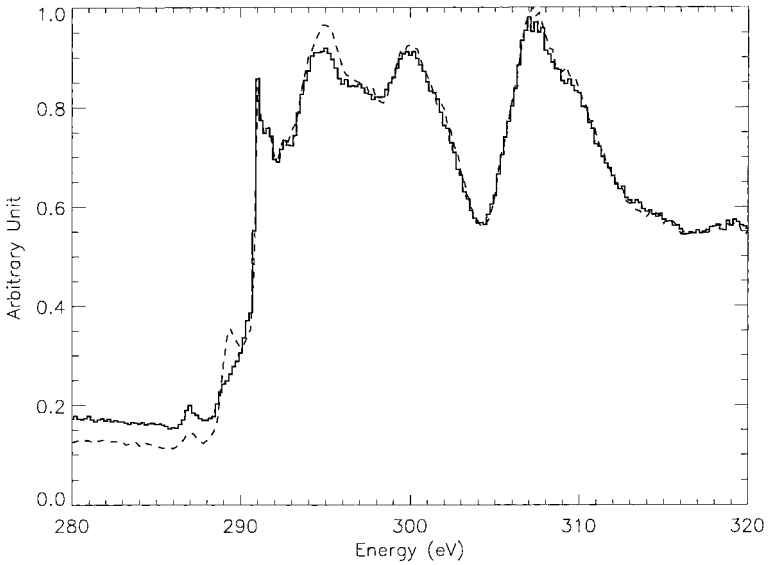

Fig. 5. Normalized channeltron counts as a function of photon energy for surface layers (PY). The dashed line corresponds to a non-processed sample, the solid line is typical of all treated samples

$I-V$ curves could not be obtained with sandwich geometries (Fig. 3b or c), the electron emission subsequent to photon interaction on the diamond surface giving rise to the creation of a charged layer that screens the electric field in the device volume.

From current measurements and wavelength calibration curves (using a GaAs photodiode), the quantum efficiency of the diamond detectors could be estimated from the

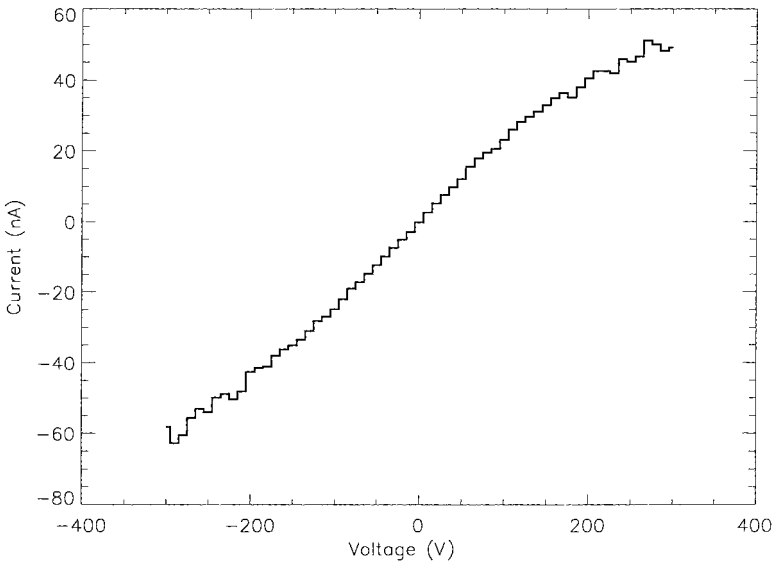

Fig. 6. Current as a function of polarization with interdigitated coplanar electrodes under monochromatic XUV flux

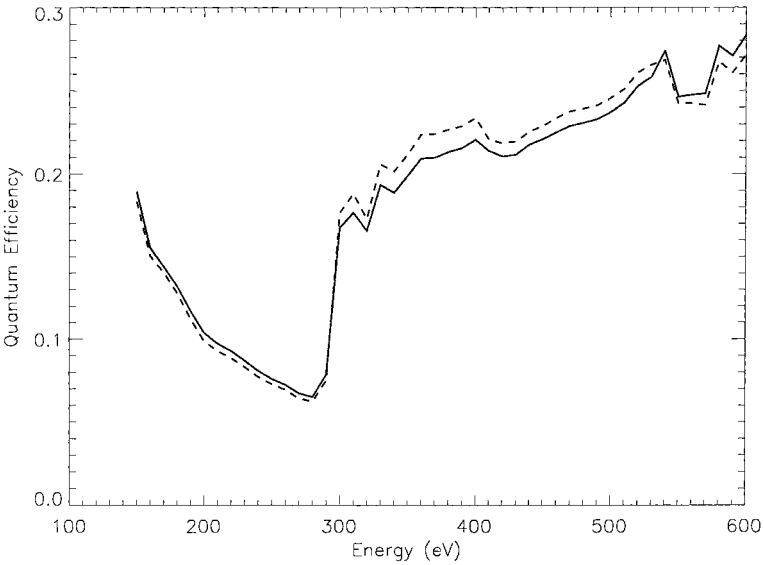

Fig. 7. QE as a function of photon energy for an interdigitated device. 50 V were applied between the electrodes. The two curves correspond to opposite polarities

following relations:

$$\Phi = \frac{i_{\mathrm{GaAs}} E_{\mathrm{GaAs}}}{e^{-} E_{\mathrm{photons}} \mathrm{QE}_{\mathrm{GaAs}}} ,$$

$$\mathrm{QE}_{\mathrm{diamond}} = \frac{i_{\mathrm{diamond}} E_{\mathrm{diamond}}}{e^{-} E_{\mathrm{photons}} \Phi} , \tag{2}$$

where Φ is the incident flux in photons per second, e^{-} the charge of the electron, E_{photons} the considered energy of the photons, $\mathrm{QE}_{\mathrm{GaAs}}$ ($\mathrm{QE}_{\mathrm{diamond}}$) the quantum efficiency of the reference diode (resp. diamond device), i_{GaAs} (i_{diamond}) the current in the reference diode (resp. diamond device), E_{GaAs} (E_{diamond}) the energy required to create a pair in GaAs (resp. diamond).

The QE plotted in Fig. 7 is defined as being the number of sensed photons per incident photon at any given photon energy. Its value does not change much whether the polarity is + or −50 V. The jump at the C_K edge is by a factor of two. This increase means that the electron is more easily collected when created in the first 100 nm than in the first 1 μm. The absolute value of the QE is three to five times smaller than in the simple model of Fig. 1. This can be explained by a loss of signal under the electrodes, photo-emission and trapping. An improved modeling is under investigation, but the point can be made already that with ≈20% QE, these are useful devices in the 200 to 600 eV range.

4. Conclusion

Although preliminary, the reported results look promising; the approach has proven useful in assessing surface properties, treatment efficiency and device behaviour. More work needs to be done, and this will happen in the following directions: the same samples will be optically characterized in the EUV using the IAS synchrotron beamline facility, and in the NUV using the LPL lasers. A new lot of optimized devices will also undergo the full

range of ultraviolet characterization, including the one described in this paper. In parallel, electrical tests and modeling will be put in correlation with the results.

Acknowledgements This project is supported by the CNES agency. The authors acknowledge the LURE for providing time on the Super-Aco synchrotron. We gratefully thank Dr. Marie-Claude Castex, Dr. Alain Deneuville, Dr. Coryn Hague, Dr. Mourad Idir, Dr. Jean-Paul Kleider, Dr. Jean Larour, Dr. Jean Manca, Dr. Denis Mencaraglia, Dr. Alessandro Mirone, Dr. Pierre Muret, Dr. Milos Nesladec and Dr. Edouard Rzepka for fruitful discussions.

References

[1] W.T. Thompson, Proc. SPIE **3764**, 196 (1999).
[2] J.-M. Defise, F. Clette, J.D. Moses, and J.-F. Hochedez, Proc. SPIE **3114**, 598 (1997).
[3] R.A. Stern, L. Shing, and M.M. Blouke, Appl. Optics **33**, 2521 (1994).
[4] NASA, AO99-OSS-04, Europa Orbiter, Pluto-Kuiper Express, Solar Probe, http://centauri.larc.nasa.gov/outerplanets/.
[5] E. Marsch et al., SOLAR ORBITER (High-resolution Mission to the Sun and Inner Heliosphere), 2000, a mission proposal in response to the ESA Call for Mission proposals for two Flexi-Missions (F2 and F3).
[6] M. Marchywka, J.-F. Hochedez, M.W. Geis, D.G. Socker, D. Moses, and R.T. Goldberg, Appl. Optics **30**, 5011 (1991).
[7] W. Jiang, J. Ahn, C.Y. Chuen, and L.Y. Loy, Rev. Sci. Instrum. **70**, 1333 (1999).
[8] M.D. Whitfield, S.S.M. Chan, and R.B. Jackman, Appl. Phys. Lett. **68**, 290 (1996).
[9] P. Bergonzo, D. Tromson, A. Brambilla, C. Mer, B. Guizard, and F. Foulon, Diamond In-line Monitors for Demanding Synchrotron Experiments, in: Proc. MRS Fall Meeting 1999 (to be published).
[10] P. Bergonzo, A. Brambilla, D. Tromson, C. Mer, C. Hordequin, B. Guizard, F. Foulon, V.A. Solé, and C. Gauthier, Diamond as a Tool for Synchrotron Radiation Monitoring: Beam Position, Profile, and Temporal Distribution, in: Proc. 10th Diamond Films Conf., Prague, Sept. 1999, to be published in Diamond Relat. Mater. (2000).
[11] P. Bergonzo, A. Brambilla, D. Tromson, C. Mer, B. Guizard, and F. Foulon, Diamond Devices as Characterisation Tools for Novel Photon Sources, in: Proc. E-MRS 1999, Strasbourg, to be published in Appl. Surf. Sci. (2000).
[12] P. Bergonzo, A. Brambilla, D. Tromson, R.D. Marshall, C. Jany, F. Foulon, C. Gauthier, V.A. Solé, A. Rogalev, and J. Goulon, Diamond Relat. Mater. **8**, 920 (1999).
[13] P. Bergonzo, A. Brambilla, D. Tromson, R.D. Marshall, C. Jany, F. Foulon, C. Gauthier, V.A. Solé, A. Rogalev, and J. Goulon, J. Synchrotron Radiat. **6**, 1 (1999).
[14] F. Foulon, P. Bergonzo, C. Borel, R.D. Marshall, C. Jany, L. Besombes, A. Brambilla, D. Riedel, L. Museur, M.-C. Castex, and A. Gicquel, J. Appl. Phys. **84**, 5331 (1998).
[15] M.C. Castex, D. Riedel, L. Museur, C. Chardonnet, A. Gicquel, F. Foulon, C. Borel, P. Bergonzo, and C. Jany, Proc. SPIE **3484**, 76 (1998).
[16] P. Dhez, E. Jourdain, O. Hainaut, J.-F. Hochedez, A. Labèque, P. Salvetat, and X-Y. Song, Proc. SPIE **3114**, 134 (1997).
[17] S.B. Dabagov, I.I. Vlasov, V.A. Murashova, M.V. Negodaev, V.G. Ralchenko, R.V. Fedorchuk, and M.N. Yakimenko, Proc. SPIE **3774**, 122 (1999).
[18] R.D. McKeag and R.B. Jackman, Proc. SPIE **3484**, 182 (1998).
[19] E. Pace, F. Galuzzi, M.C. Rossi, S. Salvatori, M. Marinelli, and P. Paroli, Nucl. Instrum. Methods A **387**, 255 (1997).
[20] C. Jany, P. Bergonzo, F. Foulon, A. Tardieu, and A. Gicquel, in: Proc. 5th Internat. Symp. Diamond Materials, Eds. J.L. Davidson, W.D. Brown, A. Gicquel, B.V. Spitsyn, and J.C. Angus, Electrochem. Soc., Inc., Pennington (NJ) 1998 (p. 208).
[21] C. Jany, F. Foulon, P. Bergonzo, and R.D. Marshall, Diamond Relat. Mater. **7**, 951 (1998).
[22] J. Vogel and M. Sacchi, J. Electron Spectroscopy **67**, 181 (1994).
[23] S. Turchini, R. Delaunay, P. Lagarde, J. Vogel, and M. Sacchi, J. Electron Spectroscopy **71**, 31 (1995).